ELSEVIER

PII: S0032-3861(98)00004-4

*Polymer* Vol. 39 No. 18, pp. 4225–4234, 1998

0032-3861/98/$19.00+0.00

# Effect of composition on orientation, optical and mechanical properties of bi-axially drawn PEN and PEN/PEI blend films

**J.C. Kim, M. Cakmak* and X. Zhou**
*Polymer Engineering Institute University of Akron, Akron OH 44325-0301, USA*
*(Received 30 September 1997; revised 3 December 1997; accepted 5 December 1997)*

The influence of biaxial deformation on the development of thermal, optical and mechanical properties of PEN and PEN/PEI blends were investigated. The refractive indices in the normal direction of biaxially stretched films decreased with the areal expansion ratio, $\lambda_{MD} \times \lambda_{TD}$. The Wide angle X-ray results showed that this is caused by the orientation of naphthalene planes that become parallel to the film surface as the expansion ratio increases. Blending PEI with PEN at concentration up to 20% was also found to reduce the naphthalene plane orientation, thereby improving the deformation behavior of PEN by eliminating highly localized neck formation attributed to this orientation behavior. The WAXS pole figure studies further indicate that biaxially oriented PEN films show bimodal ('cross-hatched') orientation of the chain axes one population in the MD1 direction and another distinct population in MD2 direction. This is also reflected in the mechanical properties where moduli exhibit equal values in MD1 and MD2 directions but lower values in other directions in the film plane. When blended with PEI at 10%–20% concentrations, the bimodal orientation is eliminated and the equal biaxially stretched films was found to exhibit in-plane isotropy. © 1998 Elsevier Science Ltd.

**(Keywords: polyethylene naphthalate; blends; biaxial stretching)**

## INTRODUCTION

Polyethylene naphthalate is relatively new polymer with good thermal, mechanical and barrier characteristics[1–3]. There are two known crystal structures of PEN. The $\alpha$ form was first identified by Mencik[4]. This form is triclinic with the cell parameters: $a = 0.651$ nm, $b = 0.575$ nm, $c = 1.32$ nm, $\alpha = 81.33°$, $\beta = 144°$, $\gamma = 100°$. The crystalline density is 1.407 g cm$^{-3}$. A different crystal structure of PEN with a higher melting point has been obtained. The unit cell of the second crystal modification (called ($\beta$) was suggested to be also triclinic with the following unit cell parameters: $a = 0.926$ nm, $b = 1.559$ nm, $c = 1.273$ nm, $\alpha = 121.6°$, $\beta = 95.57°$, $\gamma = 122.52°$, and density $\rho = 1.439$ g cm$^{-3}$. A more detailed analysis of the crystal structure formation was reported recently by Liu et al.[5]. The low temperature modification, $\alpha$, is formed at crystallization temperatures up to 200°C from the amorphous state or by rapid quenching from the melt, while the $\beta$ form is obtained by crystallizing above 240°C.

PEN exhibits neck formation upon stretching from the amorphous state at temperatures between glass transition and cold crystallization ($T_g < T_p < T_{cc}$) as discussed in our earlier papers[6,7], PEN and PEI exhibit melt miscibility in the full compositional range[8]. As a result, the increase of PEI fraction causes an increase of glass transition temperature while slightly decreasing melting point. The most important effect of adding PEI to PEN was found to be the reduction and complete elimination of neck formation in rubbery state uniaxial stretching from amorphous precursors. We have shown that this is a result of increased inter-chain friction between the PEN chains in the presence of bulky PEI chains which disrupts the cooperative alignment of naphthalene groups parallel to the surface of the films. This was found to widen the processing window where films of uniform thickness can be obtained.

In this paper, we investigate the effect of poly ether imide on the development of crystalline orientation, optical and mechanical properties of biaxially stretched PEN/PEI films.

## EXPERIMENTAL PROCEDURES

### *Sample preparation*

Polyethylene 2,6-naphthalene dicarboxylate (PEN) with intrinsic viscosity 0.86 dl g$^{-1}$ used for this study was provided in pellet form by the Eastman Kodak Company. PEI, with intrinsic viscosity 0.61 dl g$^{-1}$, was produced by the General Electric Company in pellet form (Ultem 1000). A series of PEN/PEI blends ranging in composition from 100/0 to 70/30 were prepared using a Werner & Pfleiderer co-rotating twin screw extruder (ZSK-30). The temperature along the extruder was kept at 280–290°C in order to minimize thermal cracking that occurs in PEN usually above 315°C.

### *Film preparation*

Blends were melt cast using a 1 inch single Prodex screw extruder equipped with an 8 inch wide sheet casting die and take-up device with a chill roll. The melt temperature at the die was controlled at 280°C. The films were quenched on a chill roll whose temperature was maintained at 70°C with the help of water circulating temperature control unit. The biaxial stretching experiments were performed using an Iwamoto biaxial stretcher (Model BIX 702). For stretching experiments, our earlier work[6] indicated that the optimum stretching temperature is $T_g + 20$°C. After a preheating time of about 1 h at the desired processing temperature, the undrawn cut films of 13 × 13 cm were inserted into the

* To whom correspondence should be addressed

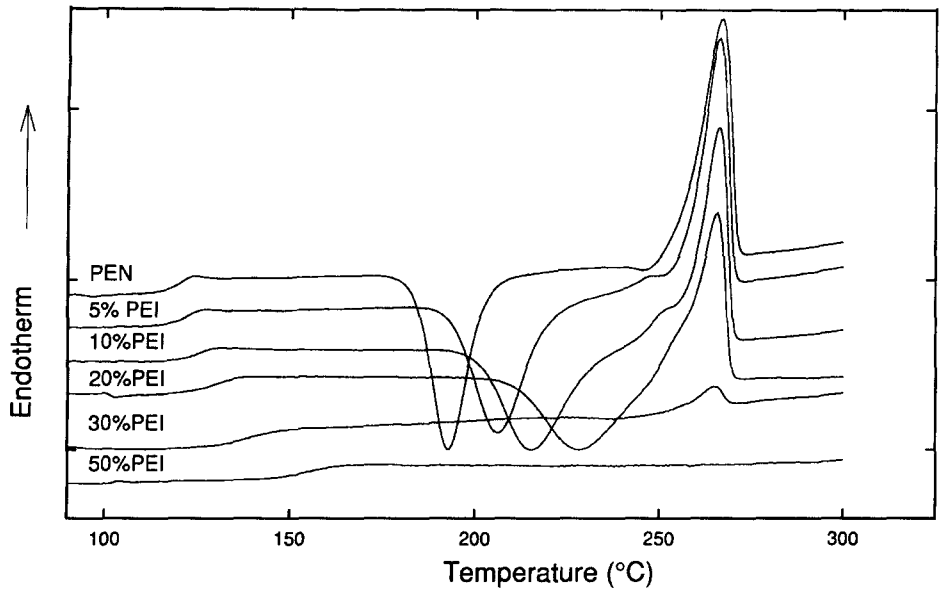


**Figure 1** The effect of composition on the d.s.c. scans of initially amorphous PEN/PEI blends

pneumatic grips of the machine. After 7 min of thermal equilibrium, the films were stretched at a stretching rate of 1200% $min^{-1}$ to the desired stretch ratios in the machine (MD), and the transverse directions (TD).

*Thermal analysis*

Thermal properties of PEN and PEN/PEI films were measured using a Perkin-Elmer differential scanning calorimeter (DSC-7). The temperature scale of the instrument was calibrated using both indium and zinc as a standard prior to each set of d.s.c. experiments. The samples of about 5 mg were crimped in standard aluminum d.s.c. pans and were scanned with a heating rate of 10°C $min^{-1}$ in a dry nitrogen atmosphere.

*Mechanical properties*

An Instron 4240 tensile tester was used to obtain the stress–strain curves of biaxially drawn films at room temperature. The test strips of 5 mm width and 6 cm length were cut in the desired directions from the interior of the processed samples. They were then tested with a gage length of 2 cm, and at a strain rate of 100% $min^{-1}$. At least three samples were tested for each condition and direction, and the results were averaged.

*Refractive indices*

Refractive indices along the three principal axes of the biaxially stretched films were measured using a Bellingham Stanley refractometer (Abbe 60/HR) with a polarizing eyepiece. At some drawing conditions, the refractive index along the MD, $n_{MD}$, was too high to be measured by the refractometer directly. This value was obtained from the refractive index in TD, $n_{TD}$, and separately measured in-plane birefringence $\Delta n_{12}$ (1 = MD and 2 = TD). This $\Delta n_{12}$ was measured with a retardation technique using a 30 order Berec compensator. A sodium lamp of wavelength 589.3 nm was used to improve measurement accuracy.

*WAXS pole figures and biaxial orientation factors*

WAXS pole figures on selected samples were taken using a GE XRD-6 X-ray generator equipped with a quarter circle goniometer. The machine was operated at 30 kV and 30 mA. Cu K$\alpha$ X-ray radiation was obtained through a detector side graphite monochromator. The samples were in the form of 2 × 2 × 2 mm cubes. These were made by successively stacking the thin blend films into layers using intermediate epoxy layers as a binder. The data was collected in step scanning mode with intervals of 10° for $\Phi$, and 5° for the azimuthal angle $\chi$, with a 20 s counting at each step.

The biaxial orientation factor, which was proposed by White and Spruiell[9], was used to evaluate the crystalline orientation. Wilchinsky's method[10–12], with a pseudo-orthorhombic model[7], was used to calculate the orientation factor of the $c$-axis and normals of naphthalene plane. Calculations are as follows:

$$c-\text{axis}: \overline{\cos^2\chi_{1u}} = 1 - 0.844\cdot\overline{\cos^2\chi_1} - 1.156\cdot\overline{\cos^2\chi_2} \quad (1)$$

$$\text{axis normal to naphthalene plane}: \overline{\cos^2\chi_{1c}}$$

$$= 1.022\cdot\overline{\cos^2\chi_1} - 0.022\cdot\overline{\cos^2\chi_2} \quad (2)$$

where $\overline{\cos^2\chi_1}$ is obtained from (100) plane; $\overline{\cos^2\chi_2}$ is obtained from (−110) plane.

## RESULTS AND DISCUSSIONS

*Thermal analysis*

The effect of composition on the thermal behavior of the amorphous blends can be observed in *Figure 1*. The increase of PEI fraction causes an increase in glass transition temperature as expected from melt miscibility and—in parallel—the breadth of the glass transition increases as well. This is particularly evident in blends containing 30% and higher PEI fraction. This suggests the presence of certain level of micro phase segregation in these blends. The increase in amplitude of the spatial concentration fluctuations can lead to such broadening of the glass transition region. The crystallizability of these blends is also influenced as judged by the location of a cold crystallization peak. The increased fraction of stiff and bulky PEI chains shifts the position of these peaks to higher temperatures. This is primarily as a result of dilution effect combined with

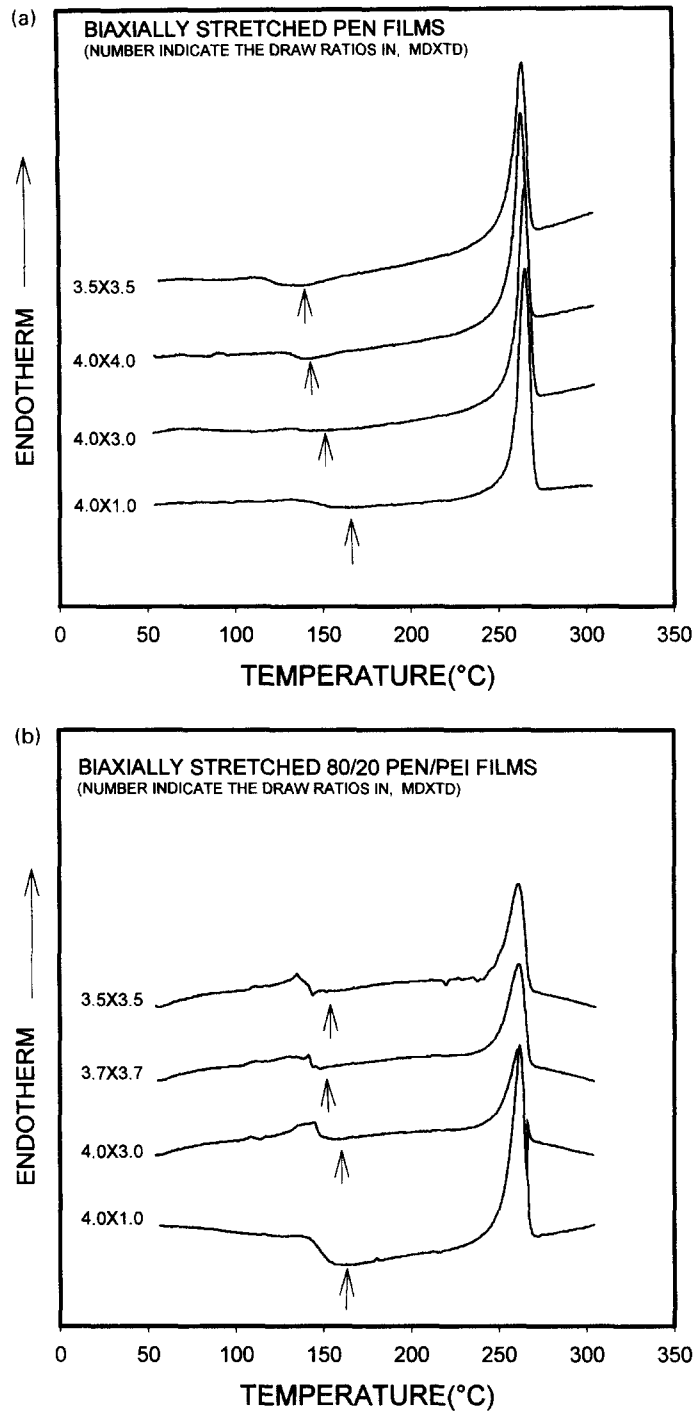


**Figure 2** (*a*) D.s.c. scans on PEN samples stretched to various stretch ratios. (*b*) D.s.c. scans on PEN/PEI samples stretched to various stretch ratios

the stiffening of the environment the crystallizable PEN chains experience at higher concentrations of PEI whose $T_g(=218°C)$ is substantially higher than that of PEN ($T_g = 120°C$). Beyond about 30% PEI concentration, the crystallizability is greatly diminished. Therefore, in this study, we decided to concentrate on the blends containing up to 20% PEI in order to preserve the crystallizability of these blends. A series of samples were stretched at their respected processing temperatures ($T_g + 20°C$) in simultaneous biaxial mode. As indicated in our previous publications, PEN stretched to low stretch ratios exhibit neck region(s) throughout the part. This limited our studies to the high deformation ratios where the films become uniform again after the disappearance of the necks which accompany strain hardening.

The d.s.c. curves for PEN and 80/20 PEN/PEI blends are shown in *Figure 2a* and *Figure 2b*, respectively, for unbalanced and balanced biaxially stretched films. At the stretch ratios presented, the cold crystallization peak is barely noticeable in the d.s.c. curves for PEN. These are indicated by arrows in the curves, as shown in *Figure 1*. With the increase of the stretch ratio, the position of this peak moves to lower temperatures. Similar observations can be made for 20% PEI blends as shown in *Figure 2b*. In these curves the cold crystallization peak occurs immediately above the glass transition temperature. The area under this peak is larger as compared to comparably processed PEN, indicating the presence of a larger percentage of oriented uncrystallized PEN chains in the blends whose crystallization was hindered by the presence of

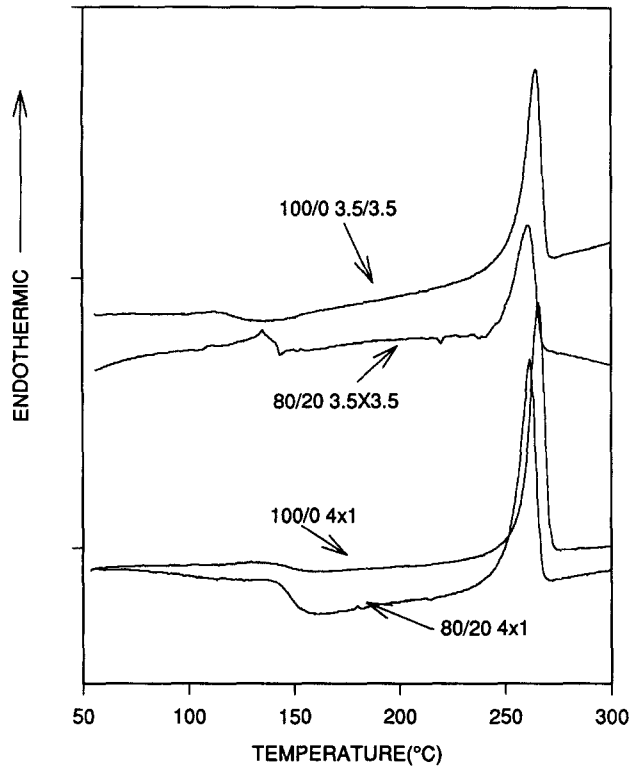


**Figure 3** D.s.c. scans of stretched films of PEN and 80/20 PEN/PEI blends

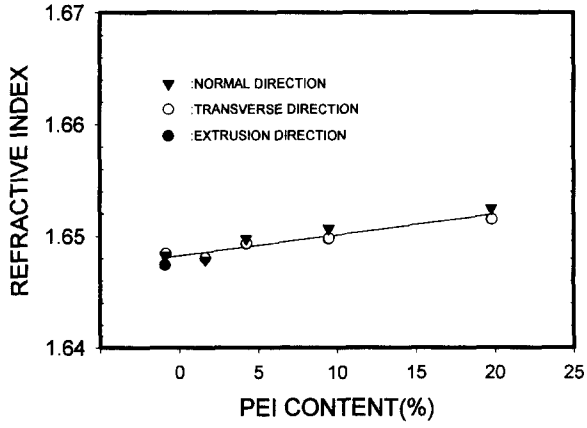


**Figure 4** Refractive indices of as-cast films of varying PEI fraction

PEI. In these films, the melting endotherm also becomes broader, particularly when the transverse direction stretch ratio is increased. A direct comparison of the d.s.c. curves in samples stretched to 4 × 1 and 3.5 × 3.5 delineate the differences caused by the presence of PEI in *Figure 3*.

*Optical properties*

The refractive indices of as-cast films increase with increased proportion of PEI as shown in *Figure 4*. The values measured in all three directions in the films are generally quite close to one another, indicating that these films are nearly optically isotropic. However, once the films are stretched, significant optical anisotropy rapidly develops as shown in *Figures 5–8*. The principal refractive indices in these graphs are plotted as a function of '*areal expansion ratio*', defined as the product of the stretch ratios in the machine and the transverse direction $\lambda_{MD} \times \lambda_{TD}$. The actual

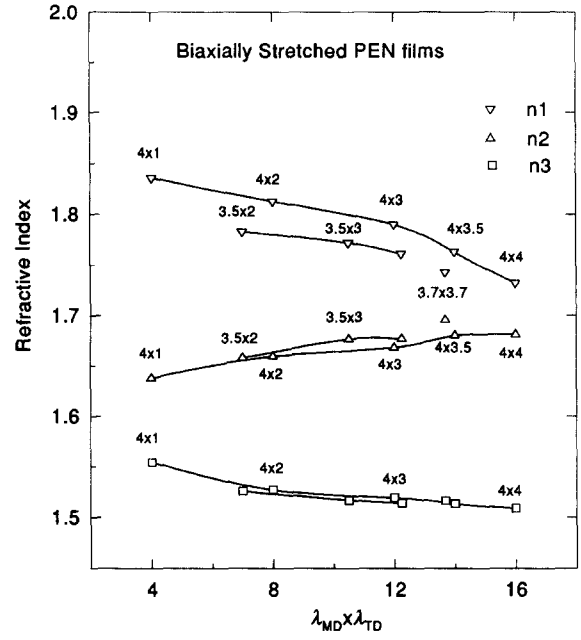


**Figure 5** Variation of principal refractive indices of biaxially stretched PEN films. Numbers in abscissa indicate the product of stretch ratios in MD and in ND (1, MD; 2, TD; 3, ND)

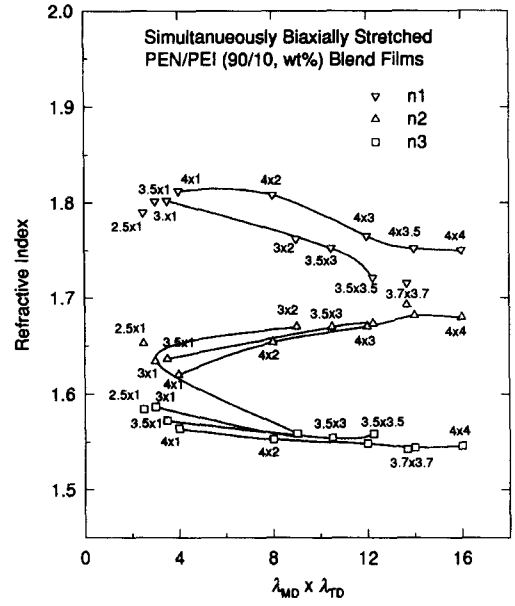


**Figure 6** Principal refractive indices of biaxially stretched 90/10 PEN/PEI blend films (1, MD; 2, TD; 3, ND)

stretch ratios in both directions are indicated next to majority of symbols.

The refractive index in the normal direction decreases as the areal expansion ratio increases. All of the refractive index data in the normal direction falls on a single line, and this indicates that the refractive index in the normal direction is dependent not on the stretching mode but on the areal expansion ratio, $\lambda_{MD} \times \lambda_{TD}$. or its equivalent inverse of the stretch ratio in the normal direction ($\lambda_{ND} = t/t_0$). The increase of transverse stretch ratio causes a decrease in the $n_1$ ( $= n_{MD}$) while increasing the $n_2$ ( $= n_{TD}$). Further, these data indicate that the refractive indices in the machine direction and the transverse direction depend not only on the expansion ratio but also on the individual stretch ratios in

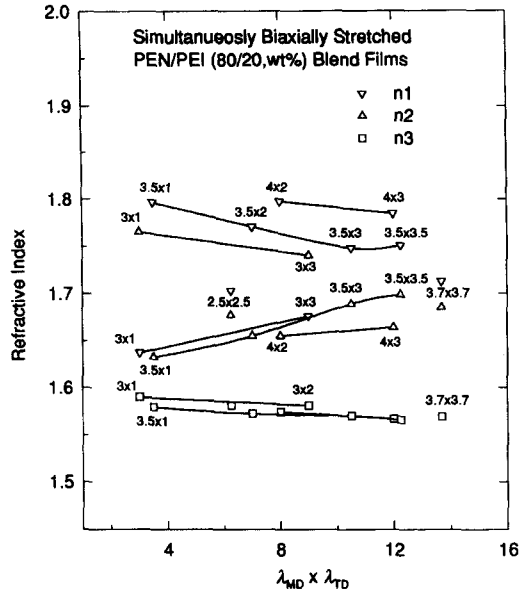


**Figure 7** Principal refractive indices of biaxially stretched 80/20 PEN/PEI blend films (1, MD; 2, TD; 3, ND)

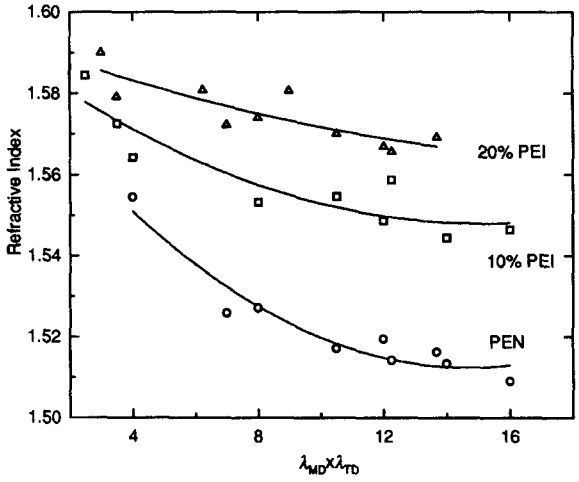


**Figure 8** Normal direction principal refractive indices of biaxially stretched films of three-blend composition as a function of the product of stretch ratios in MD with that in TD

the machine and the transverse directions, while those of the normal direction do not.

The decrease of refractive index in the normal direction with the increase in expansion ratio is caused by the re-arrangement of naphthalene rings, which become parallel to the film surface at higher expansion ratios. This is in agreement with the calculated refractive indices, assuming additivity of bond polarizabilities of PEN, as shown in *Table 1* (R. Ozisik and M. Cakmak, unpublished research). This shows the refractive index along the chain axis is highest ($n_c = 1.908$), and that normal to the naphthalene ring is the lowest ($n_n = 1.36$). This behavior is very similar to the optical properties of biaxially stretched PET films[13] where the phenyl planes preferentially orient parallel to the broad surface of the films upon stretching in biaxial mode. However, larger naphthalene groups flexibly linked along the PEN chains display this orientation much more readily under similar processing conditions as compared to the phenyl groups of PET. Interestingly, the addition of PEI to PEN influences this alignment process as partly evidenced

**Table 1** Estimated Intrinsic optical properties of PEN crystalline forms

| | Conformation[a] | |
|---|---|---|
| | *ttttt*($\alpha$) | *cttttt*($\beta$) |
| Refractive index | | |
| $n_c$ (along the chain axis) | 1.908 | 1.905 |
| $n_n$ (normal to the naphthalene plane) | 1.36 | 1.369 |
| $n_t$ (normal to the chain axis and in the naphthalene plane | 1.808 | 1.865 |
| Birefringence | | |
| $\Delta n_c^\circ = n_c - \left(\frac{n_n + n_t}{2}\right)$ | 0.324[a] | 0.288 |
| $\Delta n_{cn}^\circ = n_c - n_n$ | 0.548 | 0.536 |
| $\Delta n_{ct}^\circ = n_c - n_t$ | 0.1 | 0.04 |

[a] *t*, *trans*; *c*, *cis*

[b] In a separate study, the intrinsic birefringence of PEN was experimentally extrapolated to be around of 0.79; 100% crystalline PEN for the amorphous PEN is 0.75[17]. This discrepancy is as a result of ignoring the internal field effects in the above calculations. However, these calculations at least give us order of magnitude estimate of the differences between various directions in the crystalline lattice

in the normal direction refractive indices of 90/10 and 80/20 PEN/PEI blends shown in *Figures 6 and 7*, respectively. In these figures one can observe that there is an increased stretching mode dependency in the $n_{ND}$. Further, for the same deformation ratios the overall refractive indices in the normal direction significantly increases with the addition of PEI as demonstrated in *Figure 8*. This increase is partly caused by the increased proportion of higher refractive index PEI in the blend, and as a result of the disruption of preferential orientation tendencies of flat naphthalene groups parallel to the film surface. This last assessment cannot be concluded with the refractive index data alone, and will be substantiated using the X-ray data presented in the following sections.

### *WAXS film patterns*

*Figure 9* shows the wide-angle X-ray diffraction patterns of PEN and PEN/PEI blend films which have a 3.5 × 1.0 draw ratio. All of the observed crystalline peaks belong to the $\alpha$-form[14,15]. The differences between the two patterns indicate the absence of transverse isotropy, particularly when one examines the WAXS pattern of the pure PEN film shown in the first column. The presence of diffraction peaks in the first- and second-layer lines indicates there is a reasonable three-dimensional order in this film. Clear absence of (−110) from the WAXS patterns taken with the X-ray beam normal to the film surface and strong presence of this peak in the pattern where the beam was directed along the transverse direction, with machine direction being vertical in both patterns, indicates the presence of usual[16], very strong orientation of the naphthalene planes parallel to the surface of the film.

The addition of PEI progressively eliminates all but the strongest equatorial diffraction planes (010) observed in the pattern taken with the X-ray normal to the film surface and (−110) observed in the plane taken in the transverse direction. Particularly in the sample containing 20% PEI, the absence of higher-order peaks indicates that PEI significantly disrupts the formation of the three-dimensional lattice structure. At this high concentration of PEI, the structure approaches 'nematic-like' order with the primary order direction being in the normal direction of the films.

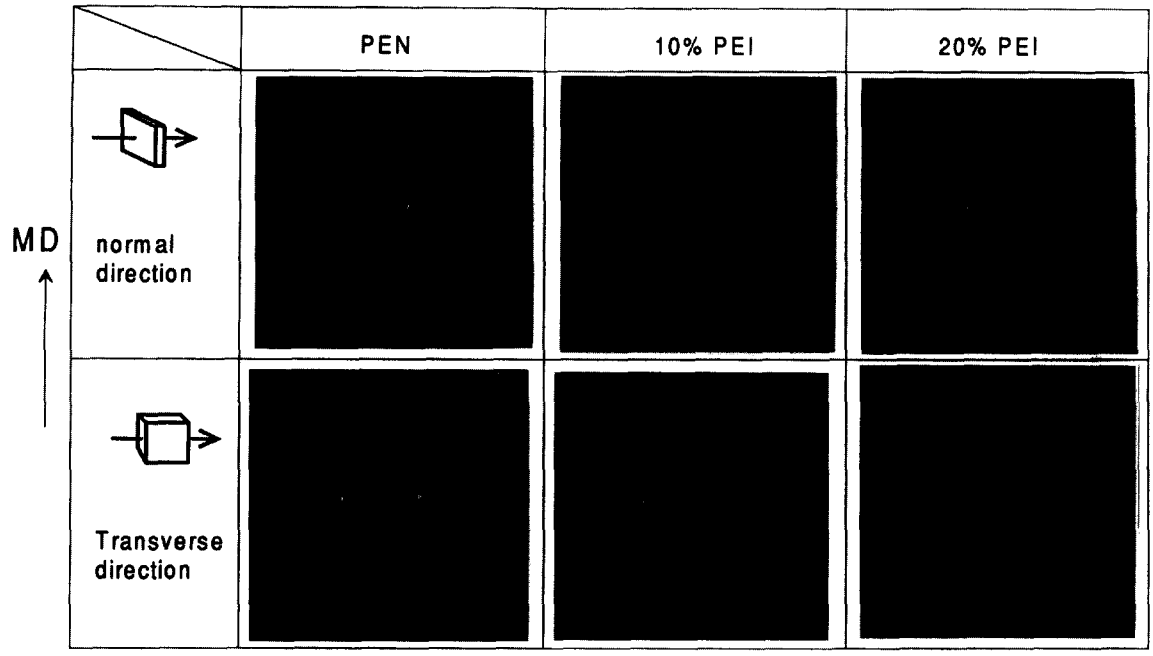


**Figure 9** WAXS patterns of PEN/PEI blend films stretched with 3.5 × 1.0 draw ratio

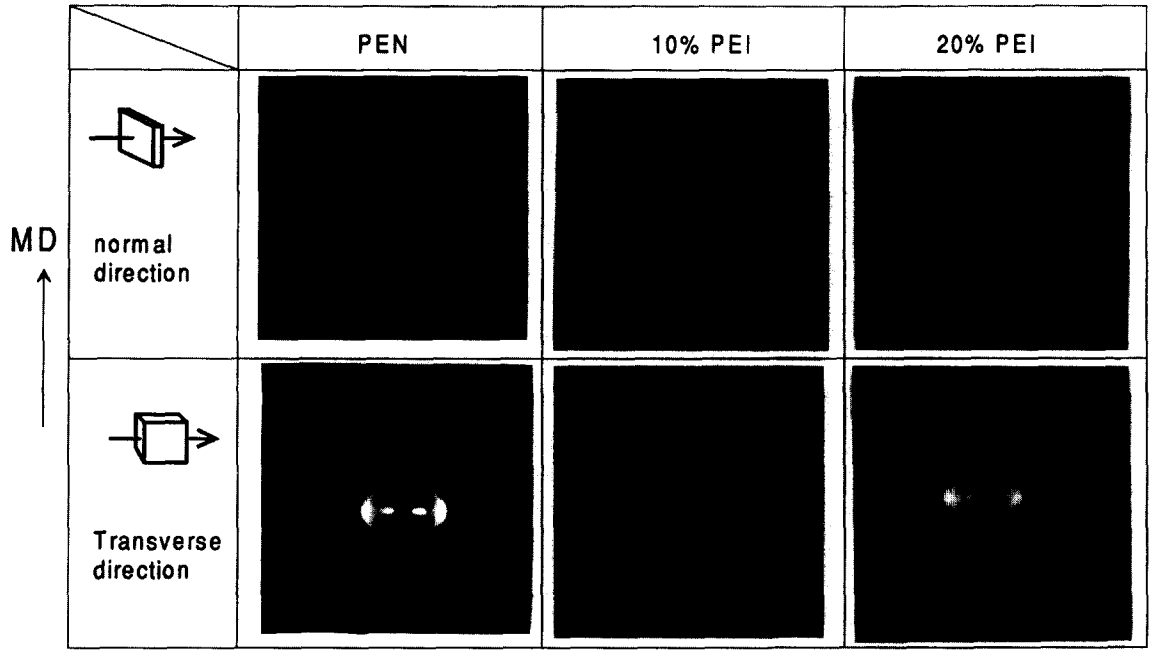


**Figure 10** WAXS patterns of PEN/PEI blend films stretched with 3.5 × 3.5 draw ratio

The WAXS patterns taken on a 3.5 × 3.5 PEN sample indicate a bimodal orientation in the strong (010) plane observed in the pattern taken with the X-rays normal to the film surface (*Figure 10*). The increase of PEI concentration to 20% leads to elimination of this bimodality, as evidenced by the uniform intensity distribution in this peak (observed as the last pattern in the top row). The absence of (−110) peaks from the top row follows the alignment of naphthalene planes parallel to the surface of the films. In this orientation these planes can only be observed when the samples are probed with the X-ray beam along the transverse direction. The quantitative discussion of the chain axes and the normals of the naphthalene planes are presented in the following section.

*WAXS pole figures*

In our earlier publication, we reported biaxially stretched PEN film bimodal chain orientation, one population oriented in the machine direction and the other in the transverse direction (or the other machine direction), even though it is stretched in the simultaneous biaxial stretching mode. The same bimodal orientation was observed in the PEN film which was simultaneously stretched with a 3.5 × 3.5 draw ratio, as shown in *Figure 11* where the pole figures of (010) planes are presented for three blend compositions. This bimodal orientation behavior arises as a result of low interchain friction when the naphthalene planes align parallel to each other and to the surface of the film. When

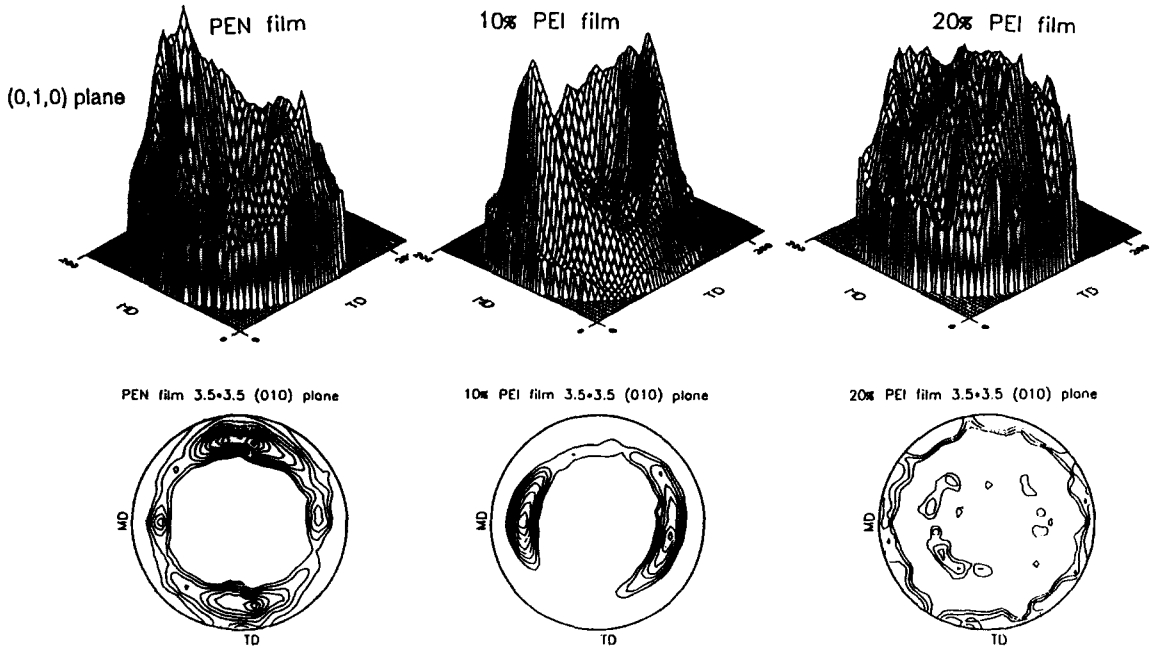


**Figure 11** Three-dimensional pole figures and isointensity contour plots of (010) planes of blend films stretched to 3.5 × 3.5 stretch ratio

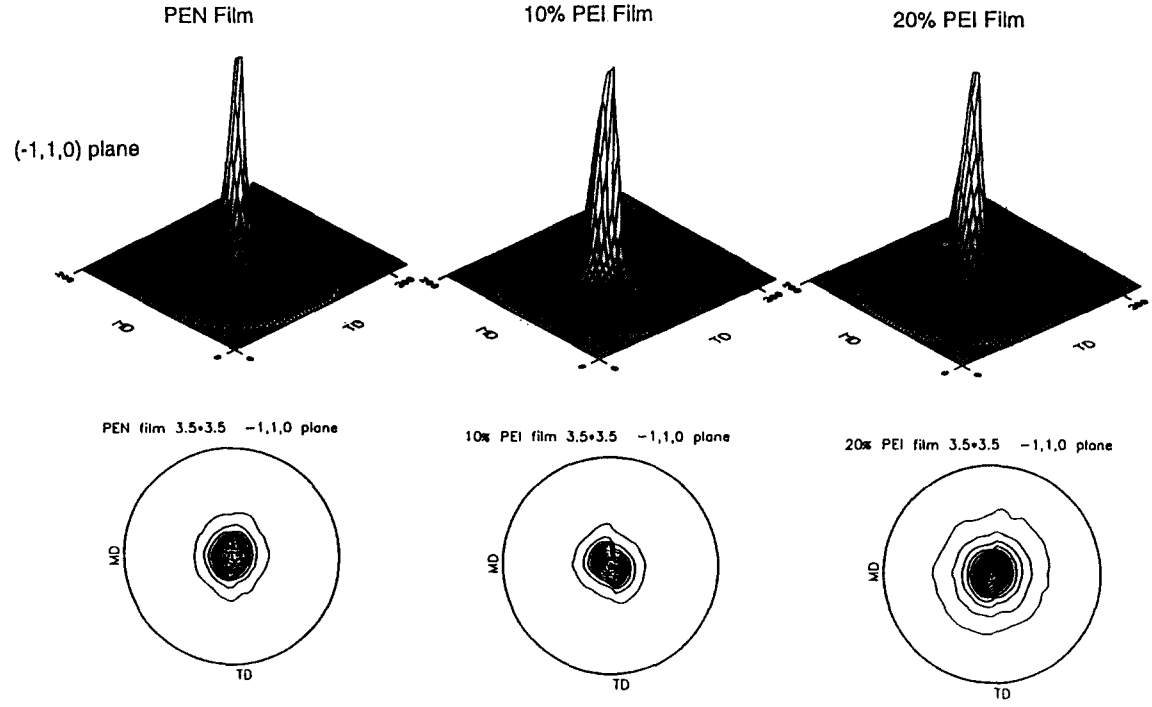


**Figure 12** Three-dimensional pole figures and isointensity contour plots of ( − 110) planes of blend films stretched to 3.5 × 3.5 stretch ratio

this 'graphitic texture' forms, the two distinct populations with their chain axes oriented in the two mutually perpendicular primary stress directions develops as little resistance to chain reorientation in the plane of the film is offered by the above texture.

As we have seen earlier in the WAXS film patterns, qualitatively this bimodal orientation slowly disappears with the increase of PEI. The ( − 110) plane poles also show very strong orientation normal to the film surface as indicated in *Figure 12*. However, one can observe that the sharpness of this orientation decreases with PEI concentration.

In order to obtain quantitative information about the effect of PEI on the crystalline orientation, White-Spruiell biaxial orientation factors were calculated from the pole figure data. *Figures 13 and 14* show the White-Spruiell biaxial orientation factors of the *c*-axis and the normal of naphthalene plane. These orientation factors for both *c*-axis and naphthalene normal axis reside along this equal biaxial line for samples stretched to 3.5 × 3.5. The increase of PEI reduces the orientation factors of the naphthalene planes (1 → 2 → 3 in the graph). While leaving the orientation factors for the chain axes (closed symbols around 0.4,0.4 coordinates) relatively unchanged (see also *Figures 14 and 15*). Similar observations can be made on samples

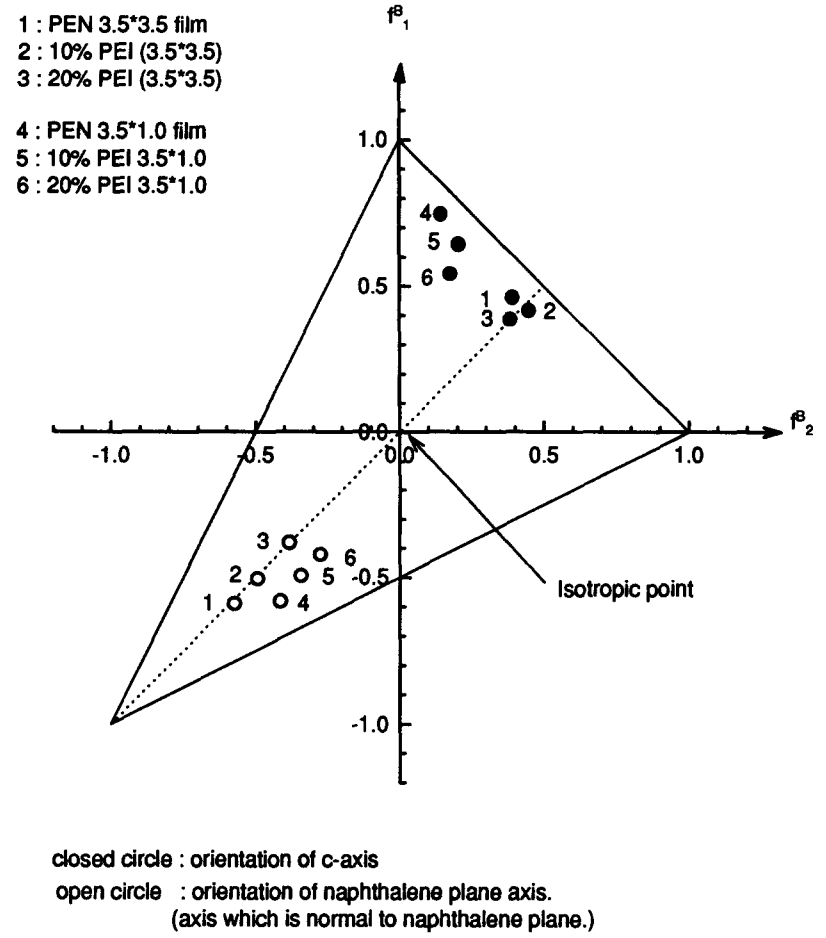


**Figure 13** White–Spruiell triangle indicating the orientation of *c*-axes and normals of naphthalene planes in films of various compositions and stretch ratios

stretched uniaxially with constrained width, as indicated in *Figure 15* with one minor difference: in these samples both orientation factors are influenced in the presence of PEI.

It should be noted that the White–Spruiell orientation factors are based on the second moment of orientation distributions and cannot distinguish between the bimodal orientation of chains and the in-plane isotropy of the chains as shown in *Figure 16d and Figure 16e*.

*Mechanical properties*

In order to ascertain the development of in-plane anisotropy with stretching and with the increase of PEI fraction, five different directions in the plane of the film (0, 22.5, 45, 65, 90°) were chosen to perform tensile tests. *Figures 17 and 18* show the in-plane anisotropy of modulus, tensile strength, and elongation at break in films stretched to $\lambda_{MD} = 4$ with different TD stretch ratios. The modulus data, which is particularly sensitive to the orientation distribution in the plane of the film, shows an unusual development of anisotropy with the transverse stretching. In 4 × 1 condition, the modulus in MD is higher than that in TD. Moduli in all directions increase as the TD stretch ratio is increased. However, in the intermediate directions (22.5, 45, 67.5°), this increase is slower than in TD. We believe that this is directly related to the bimodal orientation behavior observed in the WAXS pole figures of the biaxially stretched PEN. This effect is not as pronounced in the tensile strength values as shown in *Figure 18a*. These values do not entirely represent the original structure as they are obtained after a significant plastic deformation that occurs in testing the sample at room temperature. The elongation at

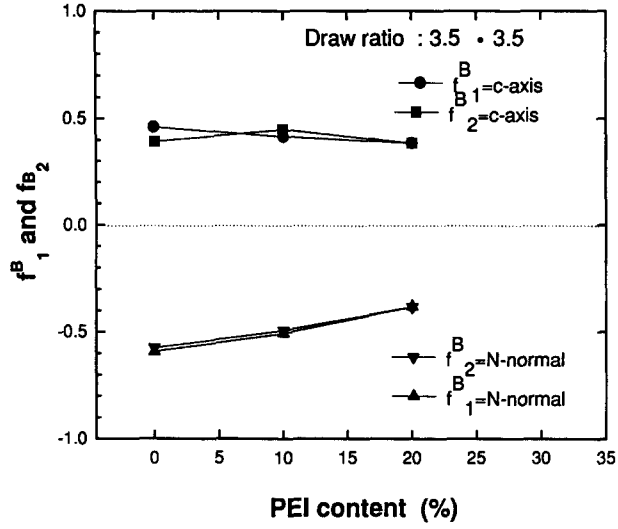


**Figure 14** White–Spruiell orientation factors of *c*-axes and normals of naphthalene planes as a function of composition. Films were stretched with a 3.5 × 3.5 draw ratio

break showed quite complex changes with deformation. When MD stretch ratio increases, the elongation at break in MD decreases, and that in TD increases first and starts decreasing with the increase of transverse stretch ratio. This behavior was also observed in the PET literature that was attributed to complex reorientation that takes place during the course of tensile testing at the intermediate testing angles. This increase in elongation at break is observed at

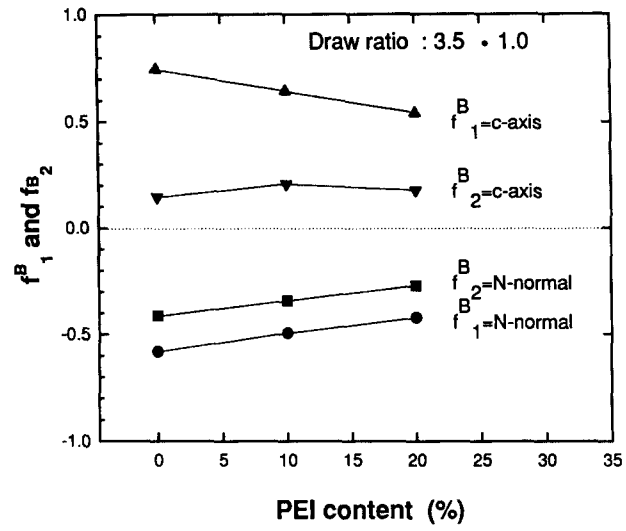


**Figure 15** White–Spruiell orientation factors of *c*-axes and normals of naphthalene planes as a function of composition. Films were stretched with a 3.5 × 1.0 draw ratio

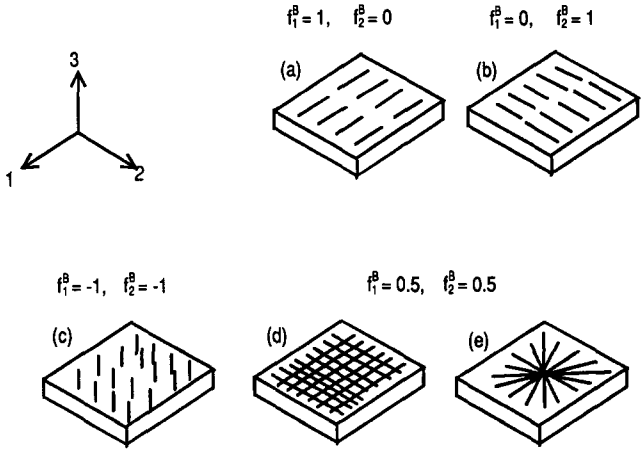


**Figure 16** Schematic illustration of the White–Spruiell orientation factor

45° in the case of PEN, and transverse direction shows very poor elongation to break at a 4 × 1 condition. This is a striking difference from behavior observed in PET. As the TD stretch increases, reasonably balanced elongation at break values are obtained in all directions in the plane of the films.

The data for the 10% PEI are presented in *Figure 19a*, *Figure 19b* and *Figure 19c* for 4 × 1, 4 × 3, and 4 × 4 conditions. As the TD stretch ratio increased, modulus and tensile strength decreased in MD but increased in all other directions without showing maxima in intermediate testing directions. Under equal biaxial conditions the samples exhibited balanced properties indicating in-plane isotropy. Comparing the moduli for 4 × 4 stretched 90/10 samples with those of PEN reveals that, although in-plane isotropy is achieved in the 90/10 blend, there is an overall decrease in modulus. This is primarily as a result of overall reduction in the orientation levels coupled with the decrease of average density with the addition of lower density PEI to the blend.

The elongation at break shows the most striking difference in the transverse testing direction (compare *Figure 18b* and *Figure 19c*). With a 10% addition of PEI, the transverse elongation at break is significantly increased,

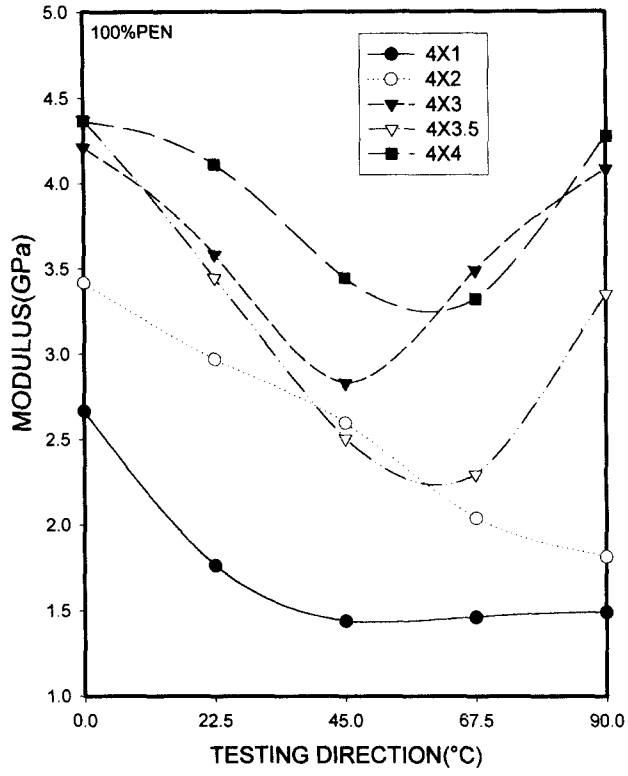


**Figure 17** The development of in-plane modulus anisotropy in stretched PEN films

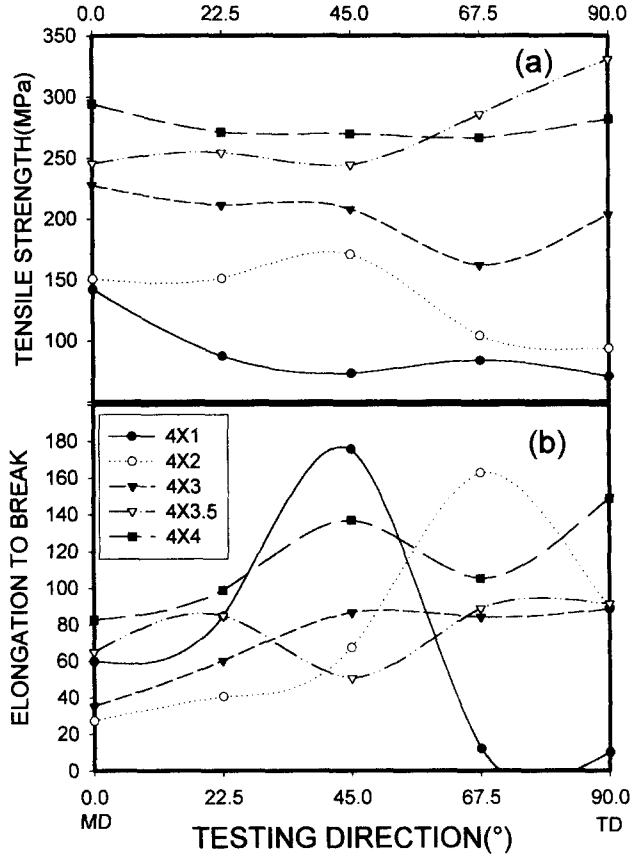


**Figure 18** The development of in-plane (*a*) tensile strength and (*b*) elongation to break anisotropy in stretched PEN films

effectively eliminating the 'splitty' character of the samples stretched under uniaxial constant width conditions. This may have significant implications on the commercial films that are stretched in unbalanced biaxial mode.

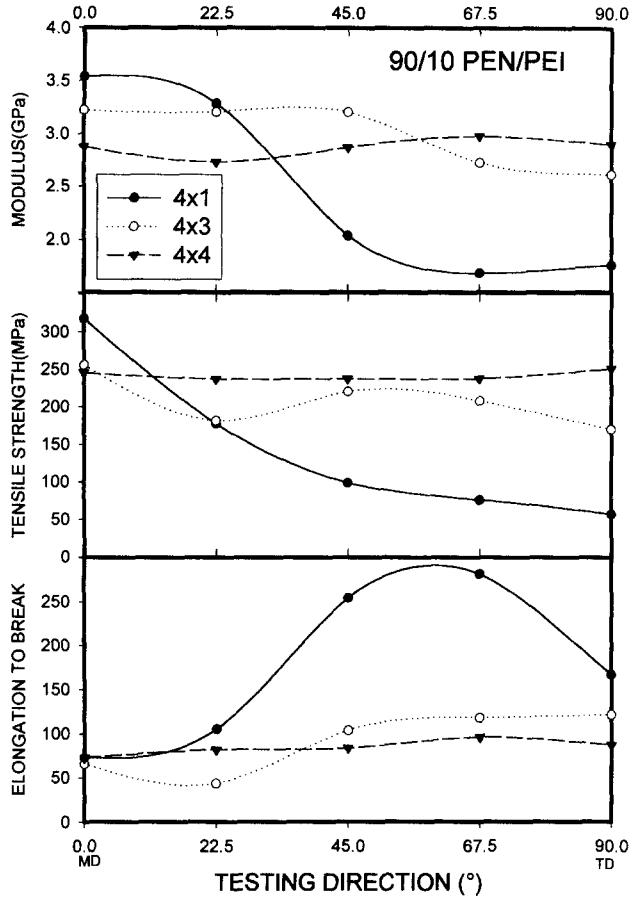


**Figure 19** The development of in-plane modulus, tensile strength and elongation to break anisotropy in stretched 90/10 PEN/PEI films

## CONCLUSIONS

The refractive indices in the normal direction of biaxially stretched films decreased as the areal expansion ratio ($\lambda_{MD} \times \lambda_{TD}$) is increased. This is due to the preferential orientation of naphthalene planes parallel to the film surface. Addition of PEI was found to reduce this preferential orientation.

Biaxially oriented PEN films shows bimodal orientation of the chain axis, one population in the machine direction and the other population in the transverse direction. Addition of as little as 10% PEI to PEN converts this bimodal ('crosshatched') orientation to 'in-plane' isotropy in the equal biaxially stretched films. This conversion of the texture is primarily as a result of increased interchain friction in the presence of stiff and bulky PEI chains that hinder the preferential orientation of the naphthalene planes parallel to one another and to the film surface. These orientation behaviors also reflected in the mechanical properties, particularly in-plane directional variation of modulus in these films. The PEN films that exhibit bimodal orientation show significantly lower moduli in directions between MD and TD (or MD2 in the equal biaxial case). The presence of PEI essentially eliminates this minimum and, under balanced biaxial conditions, the films exhibit in-plane mechanical isotropy. In addition, 90/10 PEN/PEI films also showed a higher elongation at break than PEN films in all directions, particularly under uniaxial conditions where PEN was shown to exhibit very low elongation to break in the transverse direction.

## ACKNOWLEDGEMENTS

The authors gratefully acknowledge the financial assistance provided by Eastman Kodak Company for this research.

## REFERENCES

1. Wang, Y.D., Simhambhatla, M. and Cakmak, M., *Polym. Eng. Sci.*, 1990, **30**, 721.
2. Ulcer, Y. and Cakmak, M., *Polymer*, 1994, **35**, 5651.
3. Ulcer, Y. and Cakmak, M., *J. Appl. Polym. Sci.*, 1996, **62**, 1661.
4. Mencik, Z., *Chem. Prim.*, 1967, **17**, 78.
5. J. Liu, J. Myers, P. H. Geil, J.C. Kim and M. Cakmak, *SPE Antec Tech. Paper* 43 (1997) 1562 (see also expanded paper in *J. Macromol Sci. Phys.* (in press).
6. Cakmak, M. and Kim, J.C., *J. Appl. Polym. Sci.*, 1997, **65**, 2059.
7. Cakmak, M. and Lee, S.W., *Polymer*, 1995, **36**, 4039.
8. Kim, J.C., Cakmak, M. and Geil, P.H., *SPE Antec Tech. Paper*, 1997, **43**, 1572.
9. White, J.L. and Spruiell, J.E., *Polym. Eng. Sci.*, 1981, **21**, 850.
10. Wilchinsky, Z.W., *J. Appl. Phys.*, 1959, **30**, 792.
11. Wilchinsky, Z.W., *J. Appl. Phys.*, 1960, **31**, 1969.
12. Wilchinsky, Z.W., *J. Appl. Polym. Sci.*, 1963, **7**, 923.
13. Cakmak, M., White, J.L. and Spruiell, J.E., *Polym. Eng. Sci.*, 1989, **29**, 1534.
14. Liu, J., Myers, J., Geil, P.H., Kim, J.C. and Cakmak, M., *SPE Antec Tech. Paper*, 1997, **43**, 1562.
15. Mencik, Z., *Chem. Prumysl.*, 1967, **17**, 78.
16. Murakami, S., Nishikawa, Y., Tsuji, M., Kawaguchi, A., Kohjiya, S. and Cakmak, M., *Polymer*, 1995, **36**(2), 2291.
17. Cakmak, M. and Kim, J.C., *J. Appl. Polym. Sci.*, 1997, **61**, 739.